Materials Science in Semiconductor Processing 37 (2015) 99–104

Contents lists available at ScienceDirect

Materials Science in Semiconductor Processing

journal homepage: www.elsevier.com/locate/mssp

Uniform 3D hydrothermally deposited zinc oxide nanorods with high haze ratio

Shahzada Qamar Hussain [a,e], Changzeng Yen [c], Shahbaz Khan [a], Gi Duk Kwon [a], Sunbo Kim [a], Shihyun Ahn [b], Anh Huy Tuan Le [b], Hyeongsik Park [b], S. Velumani [b,d], Junsin Yi [a,b,*]

[a] Department of Energy Science, Sungkyunkwan University, Suwon 440-746, Republic of Korea
[b] College of Information and Communication Engineering, Sungkyunkwan University, Suwon 440-746, Republic of Korea
[c] Department of Physics, Institute of Basic Science, SKKU Advanced Institute of Nanotechnology, Sungkyunkwan University, Suwon 440-746, Republic of Korea
[d] Department of Electrical Engineering (SEES), CINVESTAV-IPN, Ave Politecnico 2508, Col San Pedro Zacatenco, D.F. Mexico CP 07360, Mexico
[e] Department of Physics, COMSATS Institute of Information and Technology, Lahore 54000, Pakistan

ARTICLE INFO

Available online 26 February 2015

Keywords:
Light scattering
ZnO nanorods
Hydrothermal process
Aspect ratio
a-Si thin film solar cell

ABSTRACT

We present low cost hydrothermally deposited uniform zinc oxide (ZnO) nanorods with high haze ratios for the a-Si thin film solar cells. The problem of low transmittance and conductivity of hydrothermally deposited ZnO nanorods was overcome by using RF magnetron sputtered aluminum doped zinc oxide (ZnO:Al ~300 nm) films as a seed layer. The length and diameters of the ZnO nanorods were controlled by varying growth times from 1 to 4 h. The length of the ZnO nanorods was varied from 1 to 1.5 μm, while the diameter was kept larger than 300 nm to obtain various aspect ratios. The uniform ZnO nanorods showed higher transmittance (~89.07%) and haze ratio in the visible wavelength region. We also observed that the large diameters (> 300 nm) and average aspect ratio (3–4) of ZnO nanorods favored the light scattering in the longer wavelength region. Therefore, we proposed uniformly deposited ZnO nanorods with high haze ratio for the future low cost and large area amorphous silicon thin film solar cells.

1. Introduction

To overcome the global terawatt energy requirement, amorphous silicon (a-Si) thin film solar cells (TFSCs) have emerged as one of the future candidates for high efficiency, low cost, and large area photovoltaic devices. Light trapping is considered to be one of the essential aspects for the improvement of performance in solar cells, since it can enhance the number of photo-generated charge carriers in the absorber layer and hence reduce the overall size of the solar cell. The reduction of film thickness in a-Si TFSCs is crucial for minimizing the fabrication cost and effect of light induced degradation [1–5]. Various types of light trapping schemes are used to improve the optical and scattering characteristics of front transparent conductive oxides (TCO) films. Commonly used front TCO films for the fabrication of a-Si TFSCs include aluminum doped zinc oxide (ZnO:Al), fluorine doped tin oxide (FTO), boron doped zinc oxide (ZnO:B), and gallium doped zinc oxide (ZnO:Ga), which are deposited by magnetron sputtering, metal oxide-chemical vapor deposition (MO-CVD) or other methods requiring expensive equipment followed by separate wet chemical etching processes [6–8]. However,

* Corresponding author at: College of Information and Communication Engineering, Sungkyunkwan University, Suwon 440-746, Republic of Korea.
E-mail address: yi@yurim.skku.ac.kr (J. Yi).

http://dx.doi.org/10.1016/j.mssp.2015.02.024
1369-8001/

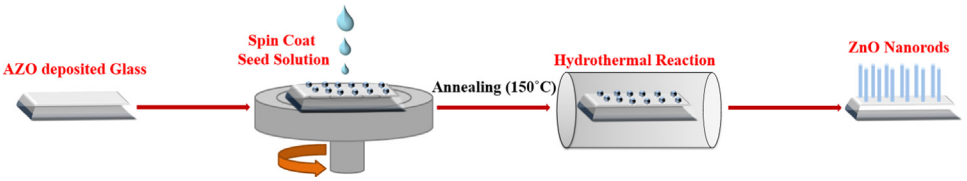

Fig. 1. Schematic diagram for the growth process of ZnO nanorods.

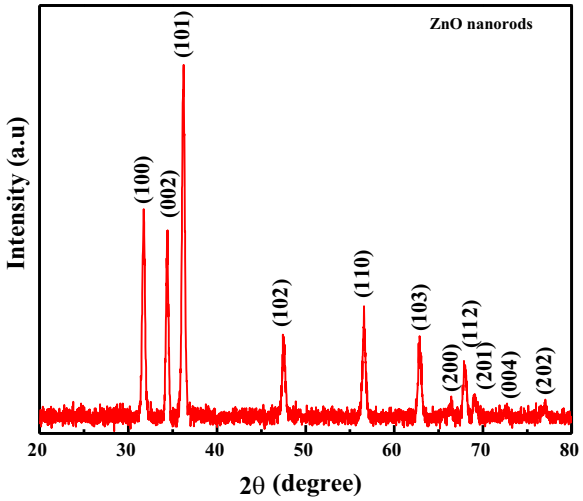

Fig. 2. X-ray diffraction (XRD) patterns of ZnO nanorods.

using these common light trapping methods, only limited size and shapes can be textured. Therefore, a novel low cost light trapping scheme is needed for large area applications. Recently, zinc oxide (ZnO) nanorods, nano-molding, and nano-dome three-dimensional (3D) arrays have been proposed for efficient light scattering in dye sensitized and a-Si thin solar cells [9–11].

ZnO nanorods can be synthesized and deposited using various methods including chemical vapor deposition (CVD), pulsed laser deposition (PLD), chemical bath deposition, aqueous solution, hydrothermal chemical processes, and electro-chemical deposition [9,12–16]. The hydrothermal process is preferred due to its simplicity, large area applications, and low cost deposition. Patil et al. reported vertically aligned ZnO nanorods thin films on steel substrate for CdS quantum dots sensitized solar cell [17]. Kilic et al. reported the fabrication of 3D ZnO nano-flower structures for high quantum and photocurrent efficiency in dye sensitized solar cells [18]. Kuang et al. reported that the ZnO nanorods structure showed better light scattering than randomly textured ZnO films for the applications of 3D nanorods solar cells [19]. Nowak et al. recently proposed low cost electro-chemically deposited ZnO nanorod arrays with high haze ratio as light trapping structures in a-Si TFSCs [9]. Ali et al. reported the novel ZnO/TiO_2-based nano/micro-hybrid heterostructures with high haze ratio for the CdS/CdSe based solar cells [23] that simultaneously offer better light scattering. Various reports have been presented related to hydrothermally deposited ZnO nanorods for dye-sensitized and CdS solar cells, however very few reports are available for the use of ZnO nanorods as a front TCO electrode with high haze ratio for a-Si TFSCs.

In this paper, we show that 3D ZnO nanorod arrays can be used as light trapping structures, additional to their front TCO behavior. We report the influence of ZnO nanorods for high transmittance, haze ratio and low sheet resistance. The surface morphologies and roughness of the ZnO nanorods are discussed for various growth times. The optical transmittance, haze ratio, and sheet resistance of ZnO nanorods are discussed and the XRD and TEM spectra of ZnO nanorods deposited on AZO glass substrates are explained. We briefly explain how these low cost large area ZnO nanorods can be used for the fabrication of a-Si thin film solar cells.

2. Experimental details

ZnO nanorods were grown on AZO based glass substrates via a solution-based hydrothermal method. Prior to the growth, the glass substrates were cleaned by rinsing with acetone, methanol, and deionized water and dried with nitrogen. A uniform AZO (300 nm) layer was deposited on the glass substrates using a RF magnetron sputtering system to improve the transmittance and conductivity of ZnO nanorods. The seed solution was prepared by dissolving 5 mM of $Zn(CH_3COO)_2 \cdot 2H_2O$ and 5 mM of KOH in anhydrous ethanol that was stirred for 10 min. The seed solution was drop cast onto AZO film, placed on a hotplate, and dried at 150 °C for 30 min to achieve good adhesion between the seed layer and AZO surface.

The ZnO nanorods were grown under synthesis conditions, where 0.025 M of hexa-methylene-tetramine (HMTA) and 0.1 M poly-ethylenimine (PEI) were added to 0.025 M of Zn $(NO3)_2 \cdot 6H_2O$ aqueous solution and stirred for 30 min. The seeded AZO substrate was then dipped into the precursor solution, followed by the hydrothermal process at 90 °C for a growth time of from 1 to 4 h. The length and diameter of ZnO nanowire arrays can be controlled by altering the growth time, the temperature, and the concentration of the precursor solution. These grown ZnO nanorod arrays were then thoroughly rinsed with DI water and dried with nitrogen gas. Fig. 1 shows the schematic diagram of the ZnO nanorods growth process.

The surface morphology of ZnO nanorods was measured by using a scanning electron microscope (SEM JEOL 7610). X-ray diffraction (XRD) analysis of ZnO nanorods was performed by using the 45 kV, 200 mA (Rigaku Smart Lab XRD, Cu Kα) system. The sheet resistance of the ZnO nanorods was characterized by using a four probe (CMT-series) system. A 3D alpha step profiler (Dektak XT) system was used to measure the rms roughness and 3D surface morphologies of ZnO nanorods deposited on the AZO glass substrates. The optical characteristics (total and diffused transmittance) were measured by using the solar cell

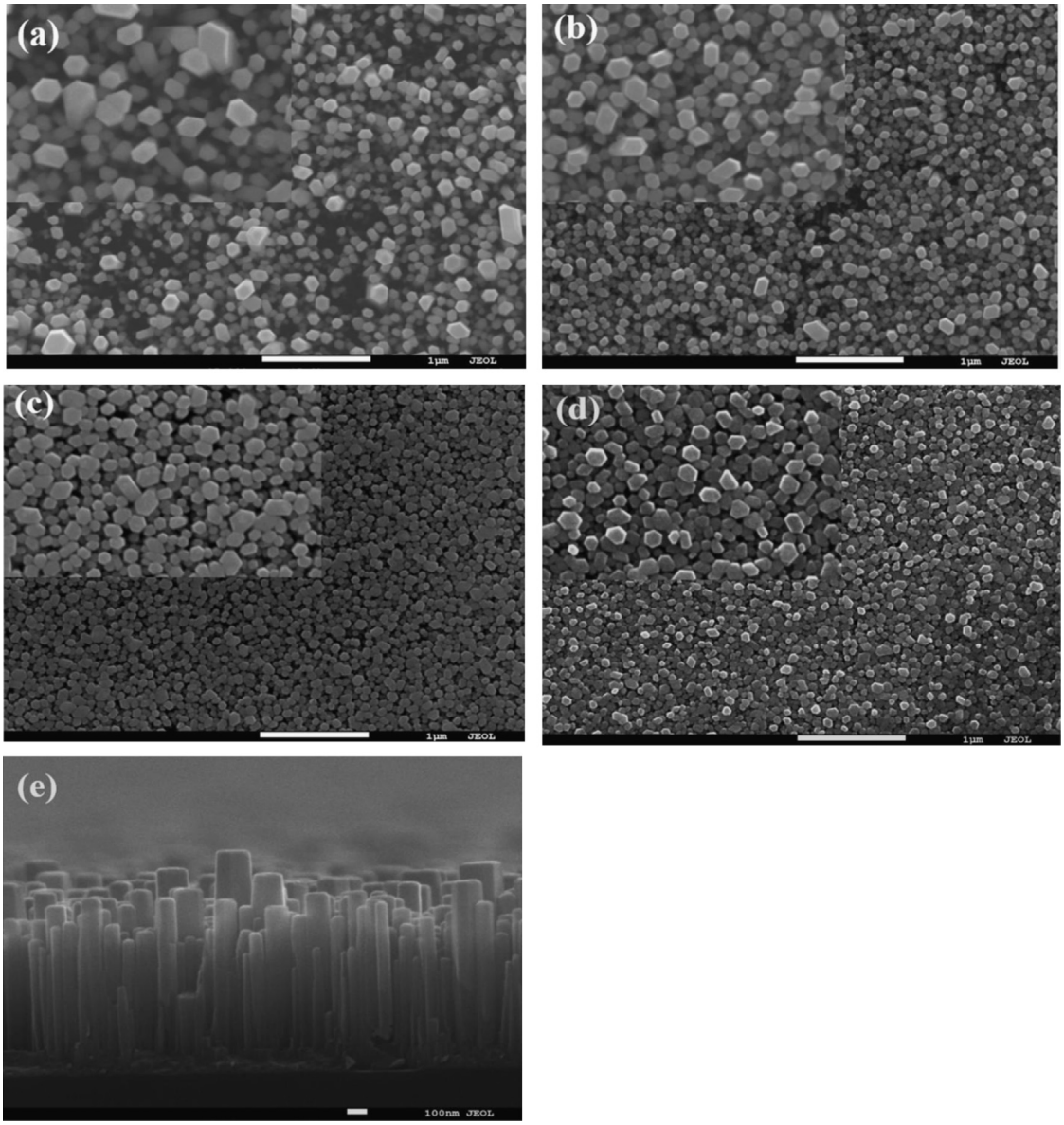

Fig. 3. SEM images of ZnO nanorods with various growth times, Top view (a) 1 h, (b) 2 h, (c) 3 h, (d) 4 h and (e) cross sectional view of ZnO nanorods.

spectral response (QE/IPCE QEX7) measurement system. The haze ratio of ZnO nanorods was calculated from the ratio of diffused to total transmittance. A high resolution transmission electron microscopic (HRTEM) analysis was performed using the JEOL, ARM200F (at 200 kV) system.

3. Results and discussion

Fig. 2 shows the X-ray diffraction (XRD) patterns of ZnO nanorods. The diffraction peaks at 31.74°, 34.38°, and 36.22° were indexed as (1 0 0), (0 0 2), and (1 0 1) planes of hexagonal wurtzite ZnO after comparing them with those in the previously published reports. The strongest peaks corresponding to the planes (0 0 2) of the ZnO nanorods showed a preferential crystal growth along the *c*-axis. [23–27]. Strong and sharp diffraction peaks of ZnO nanorods also showed good crystallinity of the samples. The presence of few other peaks such as (2 0 0), (2 0 1), (0 0 4), and (2 0 4) demonstrated that the samples obtained here were fully wurtzite structured ZnO nanorods with high crystallinity [24–26].

The surface morphology of ZnO nanorods is shown in Fig. 3. The nanorod's growth significantly depends on the seed layer and the hydrothermal deposition parameters. The magnetron sputtered AZO (~300 nm) layer was used as a seed layer to enhance the electrical conductivity. The ZnO nanorods were grown on an AZO deposited glass substrate using potassium hydroxide (KOH) concentrations with the various growth times from 1 to 4 h. It was observed that the vertically grown ZnO nanorods uniformly cover the AZO deposited glass substrate. The length and diameter of the nanorods can be controlled by

varying the reaction time, temperature, and concentration of the precursor [20]. Fig. 3(a)–(d) shows the top view of the ZnO nanorods surface morphologies for a growth time from 1 to 4 h. The vertically aligned ZnO nanorods showed average diameters of 300–400 nm, with an average length of 1.2 μm (aspect ratio ~3). The ZnO nanorods become denser with the increase of growth times from 1 to 4 h. The cross sectional view of ZnO nanorods is shown in Fig. 3 (e). The growth time plays an important role in controlling the surface morphology of ZnO nanostructures, as reported by Guo et al. [21]. Huang et al. reported that ZnO nanorods with small diameters and large lengths can improve the performance of dye sensitized solar cells [22].

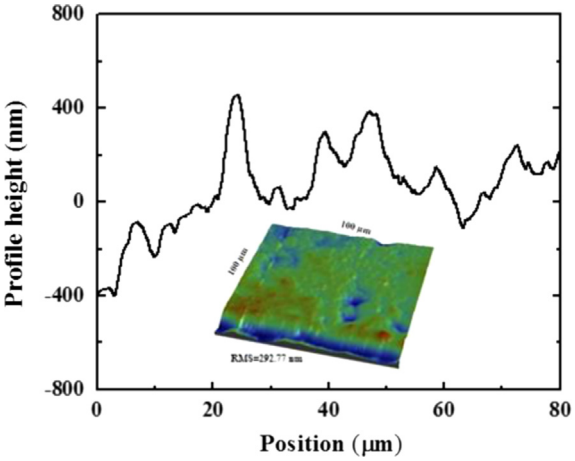

Fig. 4. Alpha step profile height of the ZnO nanorods.

The profile height and inset 3D alpha step profiler image of the ZnO nanorods are shown in Fig. 4. The roughness and 3D surface morphology of ZnO nanorods were measured by scanning a surface area of 100 × 100 μm^2. ZnO nanorods showed relatively high rms roughness of 292.77 nm. An excellent agreement was shown by the 3D profiler image and profile height of ZnO nanorods surface morphology [29–32].

Fig. 5 shows the high resolution transmission electron microscopic (HRTEM) images of ZnO nanorods. Fig. 5(b) and 5(d) shows the selected area electron diffraction (SAED) pattern of the ZnO nanorod, illustrating that the

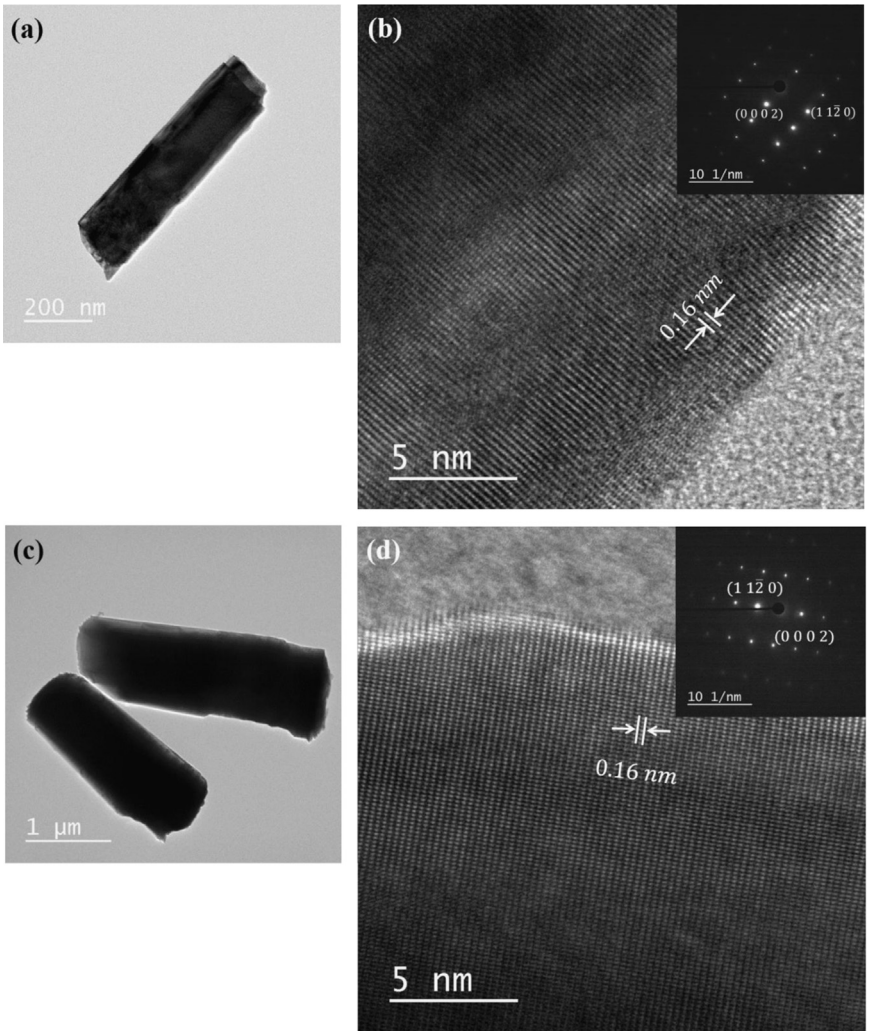

Fig. 5. Tunnelling electron microscopic (TEM) images of the ZnO nanorods.

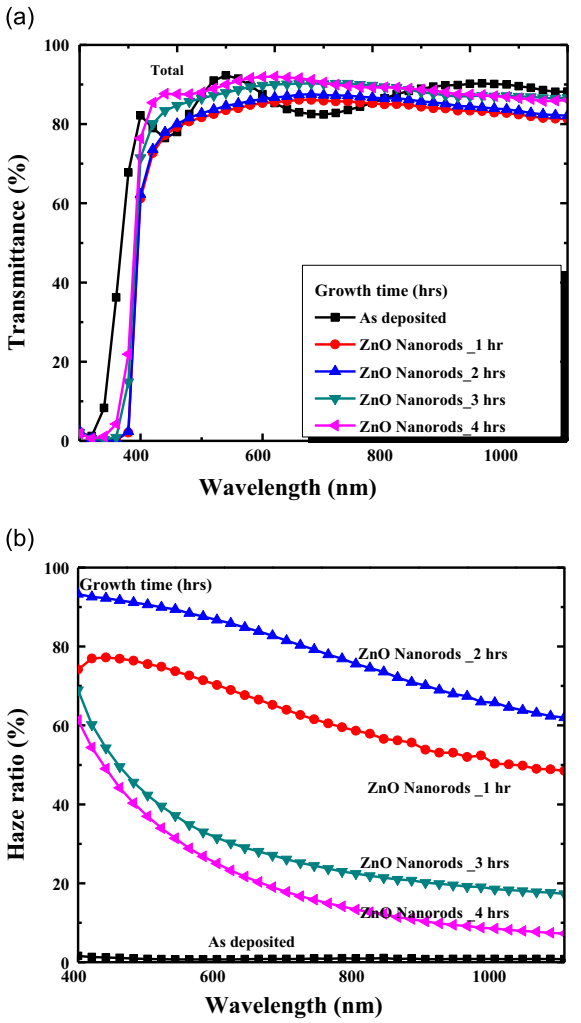

Fig. 6. Optical characteristics (a) total transmittance and (b) haze ratio of ZnO nanorods as a function of growth time.

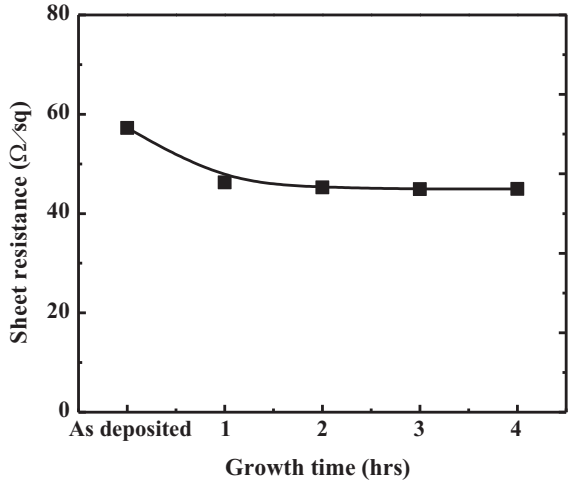

Fig. 7. Sheet resistance of the ZnO nanorods for various growth times.

individual nanorod was single crystalline in nature and preferentially grew along the [0 0 0 2] direction (the *c* axis). The sharp dark spots in the SAED pattern further confirm that the individual ZnO nanorod was single crystalline in nature. The TEM images clearly showed that the ZnO nanorods were high-quality single crystals without visible defects within the area of observation [20,24,25].

Fig. 6(a) shows the total transmittance of ZnO nanorods for various growth times. An average transmittance of about 86.53% in the visible–NIR wavelength (400–1100 nm) range was obtained for as deposited AZO film. The average total transmittance of ZnO nanorods was improved from 82.66% to 88.36% with the increase of growth time from 1 to 4 h. The haze ratio is regarded as the characteristic value for the ability of a substrate to scatter light to off-normal angles. The haze ratio of as deposited AZO film was recorded as 0.87%. The haze ratio of ZnO nanorods was improved from 62.30% to 78.21% in the visible–NIR wavelength (400–1100 nm) region with the increase of growth time from 1 to 2 h as shown in Fig. 6(b). With the further increase of growth time from 3 to 4 h, the haze ratio was slightly decreased from 29.07% to 20.86% due to the variation of ZnO nanorods surface morphology. The higher haze ratio was related to the high roughness and less dense surface morphologies resulting in greater light scattering, while the ZnO nanorods with smooth and dense surface morphologies showed less light scattering. The higher haze ratio of ZnO nanorods for the growth times of 1 and 2 h is due to the large nanorods diameter (>200 nm), since a larger structure size is beneficial for the diffuse scattering at larger wavelengths [9]. Zaera et al. showed a similar trend, whereby maximum light scattering was shown for the larger diameter of ZnO nanorods [28].

Fig. 7 shows the sheet resistance of ZnO nanorods for various growth times. The lower sheet resistance of the front TCO films is a key for the fabrication of a-Si thin film solar cells. AZO deposited glass was used as a baseline substrate for the growth of ZnO nanorods. The sheet resistance of as deposited AZO ($\sim$300 nm) film was recorded as 57.43 Ω/□, while it was decreased from 46.27 to 44.98 Ω/□ for the ZnO nanorods with the growth time from 1 to 4 h. The decrease in sheet resistance of the ZnO nanorods was mainly related to the improved crystallinity with the growth time [9,21,28]. Therefore, uniform 3D hydrothermally deposited ZnO nanorods with high haze and aspect ratios are proposed for the future low cost and large area a-Si solar cell applications.

4. Conclusion

In summary, low cost and large area uniform zinc oxide (ZnO) nanorods grown using a hydrothermal process are presented. RF magnetron sputtered AZO glass was used as a baseline substrate for the growth of ZnO nanorods with high aspect ratios. The haze ratio (78.21%) of ZnO nanorods was increased with the growth time from 1 to 2 h and then decreased due to the roughness and alignment of the ZnO nanorods. The profile height and 3D surface morphology of ZnO nanorods showed nice agreement. Sheet resistance of the ZnO nanorods was decreased from 46.27 to 44.31 Ω/□

with the increase of growth time from 1 to 4 h due to good wurtzite structure and high degree of crystallinity. Furthermore, our results revealed that the ZnO nanorods with larger diameters (>200 nm) and length (~ 2 μm) are beneficial for light scattering at wider wavelengths. Therefore, ZnO nanorods with higher light scattering properties and good electrical conductivity are proposed for future low cost and large area a-Si thin film solar cells.

Acknowledgments

This work was supported by the New & Renewable Energy Technology Development Program of the Korea Institute of Energy Technology Evaluation and Planning (KETEP) grant funded by the Korea Government Ministry of Trade, Industry & Energy (No. 20113020010010). One of the authors, S. Velumani, wishes to thank the Ministry of Science, ICT & Future Planning (MSIP) for their support (141S-6-3-0641).

References

[1] H. Tan, E. Psomadaki, O. Isabella, M. Fischer, P. Babal, R. Vasudevan, M. Zeman, A.H.M. Smets, Appl. Phys. Lett. 103 (2013) 173905.
[2] V. Jovanov, U. Palanchoke, P. Magnus, H. Stiebig, J. Hüpkes, P. Sichanugrist, M. Konagai, S. Wiesendanger, C. Rockstuhl, D. Knipp, Opt. Express 21 (2013) A595–A606.
[3] S.Q. Hussain, S. Ahn, H. Park, G. Kwon, J. Raja, Y. Lee, N. Balaji, H. Kim, A.H.T. Le, J. Yi, Vacuum 94 (2013) 87–91.
[4] S.T. Hwang, C.B. Park, Trans. Electr. Electron. Mater. 11 (2010) 81–84.
[5] S.Q. Hussain, S. Kim, S. Ahn, N. Balaji, Y. Lee, J.H. Lee, J. Yi, Sol. Energy Mater. Sol. Cells 122 (2014) 130–135.
[6] H. Park, J. Lee, H. Kim, D. Kim, J. Raja, J. Yi, Appl. Phys. Lett. 102 (2013) 191602–191605.
[7] B. Janthong, Y. Moriya, A. Hongsingthong, P. Sichanugrist, M. Konagai, Sol. Energy Mater. Sol. Cells 119 (2013) 209–213.
[8] A. Hongsingthong, T. Krajangsang, B. Janthong, P. Sichanugrist, M. Konagai, in: Proceedings of the 37th IEEE Photovoltaic Specialists Conference (PVSC), 2011, pp. 000791–000794.
[9] R.E. Nowak, M. Vehse, O. Sergeev, K. Maydell, C. Agert, Sol. Energy Mater. Sol. Cells 125 (2014) 305–309.
[10] C. Battaglia, J. Escarre, K. Soderstrom, M. Charriere, M. Despeisse, F.J. Haug, C. Ballif, Nat. Photonics 5 (2011) 535–538.
[11] J. Zhu, C.-M. Hsu, Z. Yu, S. Fan, Y. Cui, Nano Lett. 10 (2010) 1979–1984.
[12] X. Liu, X. Wu, H. Cao, R.P.H. Chang, J. Appl. Phys. 95 (2004) 3141–3147.
[13] S. Choopun, H. Tabata, T. Kawai, J. Cryst. Growth 274 (2005) 167–172.
[14] R. Shabannia, H.A. Hassan, Mater. Lett. 90 (2013) 156–158.
[15] N. Lepot, M.K.V. Bael, H.V.D. Rul, J. D'Haen, R. Peeters, D. Franco, J. Mullens, Mater. Lett. 61 (2007) 2624–2627.
[16] I. Shakir, Z. Ali, J. Bae, J. Park, D.J. Kang, RSC Adv. 4 (2014) 6324–6329.
[17] S.B. Patil, A.K. Singh, Electrochim. Acta 56 (2011) 5693–5701.
[18] B. Kilic, T. Günes, I. Besirli, M. Sezginer, S. Tuzemen, Appl. Surf. Sci. 318 (2014) 32–36.
[19] Y. Kuang, K.H.M. van der Werf, Z.S. Houweling, M.D. Vece, R.E. I. Schropp, J. Non-Cryst. Solids 358 (2012) 2209–2213.
[20] M. Raja, N. Muthukumarasamy, D. Velauthapillai, R. Balasundaraprabhu, S. Agilan, T.S. Senthil, Sol. Energy 106 (2014) 129–135.
[21] M. Guo, P. Diao, S. Cai, J. Solid State Chem. 178 (2005) 1864–1873.
[22] Q. Huang, L. Fang, X. Chen, M. Saleem, J. Alloy. Compd. 509 (2011) 9456–9459.
[23] Z. Ali, I. Shakir, D.J. Kang, J. Mater. Chem. A 2 (2014) 6474–6479.
[24] L.Y. Lin, M.H. Yeh, C.P. Lee, C.Y. Chou, R. Vittal, K.C. Ho, Electrochim. Acta 62 (2012) 341–347.
[25] X. Liu, X. Wu, H. Cao, R.P.H. Chang, J. Appl. Phys. 95 (2004) 3141–3147.
[26] Y. Kuang, K.H.M. van der Werf, Z.S. Houweling, M.D. Vece, R.E. I. Schropp, J. Non-Cryst. Solids 358 (2012) 2209–2213.
[27] Z. Ali, S.N. Cha, J.I. Sohn, I. Shakir, C. Yan, J.M. Kim, D.J. Kang, J. Mater. Chem. 22 (2012) 17625–17629.
[28] R.T. Zaera, J. Elias, C.L. Clément, Appl. Phys. Lett. 93 (2008) 233119–233122.
[29] M.L. Addonizio, A. Spadoni, A. Antonaia, Appl. Surf. Sci. 287 (2013) 311–317.
[30] F.H. Wang, C.F. Yang, Y.H. Lee, Nanoscale Res. Lett. 9 (2014) 97–103.
[31] W.T. Yen, Y.C. Lin, J.H. Ke, Appl. Surf. Sci. 257 (2010) 960–968.
[32] J. Raja, K. Jang, S.Q. Hussain, S. Chatterjee, S. Velumani, N. Balaji, J. Yi, Appl. Phys. Lett. 106 (2015) 033501–033504.